Recombination rates, Resonance Strengths and Line Profiles of Dielectronic Satellite Lines of He-like Ca, Fe, Ni

Sultana N. Nahar[1], Justin Oelgoetz[2] and Anil K. Pradhan[1]

[1] Department of Astronomy, The Ohio State University, Columbus, OH 43210, USA nahar@astronomy.ohio-state.edu, pradhan@astronomy.ohio-state.edu
[2] Los Alamos National Laboratory, X-1-NAD, Box 1336, Mail Stop F663, Los Alamos, NM 87545, USA, oelgoetz@lanl.gov

Summary. Dielectronic satellite (DES) lines arising from the radiative decay of ions with excited cores are used as diagnostics of the plasma conditions found in astronomical objects. In collisional plasmas, the most common DES lines are due to an electron being dielectronically captured by a He-like ion, forming a 3-electron, Li-like ion in a doubly excited, autoionizing state (i.e. 1s2l2l' (KLL), 1s2l3l' (KLM), etc). These states can decay to bound levels by emitting a photon, completing a process known as dielectronic recombination (DR). The autoionizing KLL complex gives rise to 22 DES lines, labeled 'a' through 'v', via transitions of the type $1s2l2l' \rightarrow 1s^2 2l$. These lines are seen at energies lower than the He-like resonance line ($1s2p(^1P_1^0) \rightarrow 1s^2(^1S_0)$ - which is also referred to as the 'w' line). The unified recombination method, which treats photoionization and electron-ion recombination in a manner which couples autoionizing states to the continuum, has been extended to study the DES lines of the highly charged ions Ca XVIII, Fe XXIV, and Ni XXVI. In contrast to obtaining a single energy point for a DES line (as is the case for existing theoretical approaches based on the isolated resonance approximation - IRA), the unified method: (i) provides detailed profiles of DES lines, including the blending of lines which occurs in nature, (ii) includes the background contribution of radiative recombination (RR), and (iii) provides a simple relation between the resonance strengths and recombination rates of narrow lines which is useful for astrophysical modeling.

1 Introduction and Theory

There are two ways of measuring DES lines: (i) the related quantities of satellite line intensity (I_s) and the intensity ratio ($\frac{I_s}{I_w}$), and (ii) the resonance strength, S. These are defined as follows:

$$I_s \approx \alpha_s \frac{n_i}{n_e} \quad , \quad \frac{I_s}{I_w} \approx \frac{\alpha_s}{q_w} \ , \ \text{and} \ S = \int_{E_i}^{E_f} \sigma_{RC} \, d\epsilon \tag{1}$$

M. Chávez Dagostino et al. (eds.), *New Quests in Stellar Astrophysics II*, Astrophysics and Space Science Proceedings, DOI 10.1007/978-0-387-87621-4_35,

where α_s is the recombination rate coefficient through the DES line, n_i is the ion density, q_w is the collisional excitation rate coefficient of the w-line, E_i and E_f are the lower an upper bounds of the line shape, and σ_{RC} the recombination cross section (e.g. Beiersdorfer et al. 1992).

The earlier theoretical treatments, initiated by Gabriel (1972), are based on the IRA. For a continuum electron that is captured into autoionizing state i by an ion in state m which then decays to state j the recombination rate coefficient (Bates & Dalgarno 1962) is calculated as

$$\alpha_s^{DR}(T) = \frac{g_i}{2g_m}\frac{h^3 e^{\frac{-\epsilon_s}{kT}}}{(2\pi m_e kT)^{\frac{3}{2}}}\frac{A_a(i\rightarrow m)A_r(i\rightarrow j)}{\sum\limits_l A_r(i\rightarrow l)+\sum\limits_k A_a(i\rightarrow k)}\ , \tag{2}$$

where A_r is the radiative decay rate, and A_a the autoionization rate. The IRA does not include the background RR contribution or interference effects, although these may be small.

The unified method (Nahar & Pradhan 1994; Zhang et al. 1999) calculates σ_{RC} from detailed photoionization cross sections (σ_{PI}) that include autoionizing resonances:

$$\sigma_{RC} = \sigma_{PI}\frac{g_i}{g_j}\frac{h^2\omega^2}{4\pi^2 m^2 c^2 v^2}. \tag{3}$$

The satellite lines are the resonances in σ_{RC} and their structures provide the energy profile of DES lines and include the contribution of the background and interference effects. Thus the entire DES spectrum is generated naturally.

The needed cross sections are calculated using the relativistic Breit-Pauli R-matrix (BPRM) method which includes coupling between channels (Nahar & Pradhan 2006). The recombination rate coefficient of a DES line is obtained from the above using the following expression:

$$\alpha_R(T) = \frac{4}{\sqrt{2\pi m}}\frac{1}{(kT)^{3/2}}\int_{E_i}^{E_f}\epsilon\ e^{-\frac{\epsilon}{kT}}\sigma_{RC}d\epsilon\ . \tag{4}$$

For a narrow resonance line we can approximate the electron distribution as a constant over the line's width. Taking ϵ_s to be the line's peak energy, we can write

$$\alpha_s(T) = \frac{4}{\sqrt{2\pi m}}\frac{e^{-\frac{\epsilon_s}{kT}}}{(kT)^{3/2}}\int_{E_i}^{E_f}\epsilon\ \sigma_{RC}d\epsilon = f(T)S_{RC} \tag{5}$$

where

$$S_{RC}(s) = \int_{E_i}^{E_f}\epsilon\ \sigma_{RC}d\epsilon\ \text{ and }\ f(T) = \frac{4}{\sqrt{2\pi m}}\frac{e^{-\frac{\epsilon_s}{kT}}}{(kT)^{3/2}} = 0.015484\frac{e^{-\frac{\epsilon_s}{kT}}}{T^{3/2}}. \tag{6}$$

Hence, the recombination rate coefficient of the DES line s can be written as

$$\alpha_s(T) = S_{RC} f(T) \ . \tag{7}$$

S_s can be approximated from $S_{RC}(s)$ as $S(s) = S_{RC}(s)/\epsilon_s$.

Since previous methodologies employ the IRA (e.g. Bely-Dubau et al. 1982; Vainshtein & Safronova 1978) most modeling codes calculate these line intensities using equation (2) . A correspondence between the present and the earlier approaches can be established by formulating the autoionization rates (A_a) from unified resonance strengths. Approximating $\alpha_s^{DR}(T)$ by $\alpha_s(T)$, it can be shown for KLL lines that:

$$A_a(i \to m) = \frac{S_{RC}}{\frac{g_i}{g_m}\frac{h^3}{16\pi m_e} A_r(i \to j) - S_{RC}} \sum_l A_r(i \to l) \ . \tag{8}$$

2 Results

Figure 1 presents the theoretical satellite spectrum of Fe XXIV. The energy profile of the DES lines can be seen clearly. In the top panel, which shows the total spectrum, not all of the 22 lines can be distinguished due to blending of DES lines. The individual lines are isolated in the lower panels by breaking the σ_{RC} into contributions from individual $J\pi$. It should be noted that the BPRM method can not identify the spectroscopic assignment of a resonance a priori. Thus, due to natural overlapping among resonance profiles, it is necessary to

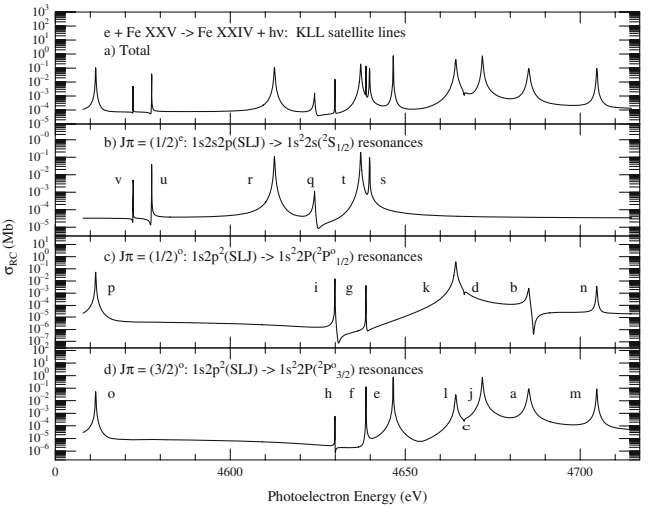

Fig. 1. DES lines of KLL complex of Fe XXIV: a) shows the total spectrum, b-d) show resolved and identified individual lines from three recombined bound levels (b) $1s^2 2s(^2S_{1/2})$, (c) $1s^2 2p(^2P^o_{1/2})$, (d) $1s^2 2p(^2P^o_{3/2})$.

Table 1. The 22 KLL DES lines: Energy positions E (eV) for Fe, Ni, and Ca along with strengths S (in 10^{-20}cm^{2}eV) for Fe.

Key	Transition	E_{Expt} eV	E_{th} eV	S(s)	S_{RC}	E_{th} eV	E_{th} eV
		Fe				Ni	Ca
1 o	$1s2s^2(^2S_{1/2}) \rightarrow 1s^22p(^2P^o_{3/2})$	4553.4	4561.53	0.8832	1.034	5299.32	2678
2 p	$1s2s^2(^2S_{1/2}) \rightarrow 1s^22p(^2P^o_{1/2})$	4553.4	4561.54	0.8820	1.033	5299.32	2678
3 v	$1s2p^3P^o2s(^4P^o_{1/2}) \rightarrow 1s^22s(^2S_{1/2})$	4573.9	4572.19	0.0599	0.0703	5312.25	2686
4 u	$1s2p^3P^o2s(^4P^o_{3/2}) \rightarrow 1s^22s(^2S_{1/2})$	4578.9	4577.52	0.1628	0.1913	5319.17	2688
5 r	$1s2p^1P^o2s(^2P^o_{1/2}) \rightarrow 1s^22s(^2S_{1/2})$	4615.1	4612.63	3.798	4.495	5358.17	2716
6 q	$1s2p^1P^o2s(^2P^o_{3/2}) \rightarrow 1s^22s(^2S_{1/2})$	4625.3	4622.54	0.0819	0.0972	5372.30	2719
7 i	$1s2p^2(^4P_{1/2}) \rightarrow 1s^22p(^2P^o_{1/2})$	4624.6	4629.91	0.0785	0.0933	5379.37	2726
8 h	$1s2p^2(^4P_{1/2}) \rightarrow 1s^22p(^2P^o_{3/2})$	4624.6	4629.92	0.0055	0.0066	5379.37	2726
9 t	$1s2p^3P^o2s(^2P^o_{1/2}) \rightarrow 1s^22s(^2S_{1/2})$	4632.9	4635.60	5.517	6.564	5387.31	2729
10 g	$1s2p^2(^4P_{3/2}) \rightarrow 1s^22p(^2P^o_{1/2})$	4639.4	4638.77	0.0120	0.0143	5392.41	2729
11 f	$1s2p^2(^4P_{3/2}) \rightarrow 1s^22p(^2P^o_{3/2})$	4632.9	4638.77	0.3721	0.4430	5392.41	2729
12 s	$1s2p^3P^o2s(^2P^o_{3/2}) \rightarrow 1s^22s(^2S_{1/2})$	4642.5	4639.79	1.291	1.538	5392.30	2731
13 e	$1s2p^2(^4P_{5/2}) \rightarrow 1s^22p(^2P^o_{3/2})$	4639.0	4646.57	0.4849	5.783	5402.16	2732
14 k	$1s2p^2(^2D_{3/2}) \rightarrow 1s^22p(^2P^o_{1/2})$	4658.1	4664.43	17.43	20.85	5419.96	2747
15 l	$1s2p^2(^2D_{3/2}) \rightarrow 1s^22p(^2P^o_{3/2})$	4658.1	4664.43	1.445	1.729	5419.96	2749
16 d	$1s2p^2(^2P_{1/2}) \rightarrow 1s^22p(^2P^o_{1/2})$	4658.6	4667.21	0.7809	0.9354	5421.21	2751
17 c	$1s2p^2(^2P_{1/2}) \rightarrow 1s^22p(^2P^o_{3/2})$	4658.6	4666.78	0.1703	0.2040	5421.21	2747
18 j	$1s2p^2(^2D_{5/2}) \rightarrow 1s^22p(^2P^o_{3/2})$	4664.1	4672.05	26.82	32.18	5432.44	2749
19 a	$1s2p^2(^2P_{3/2}) \rightarrow 1s^22p(^2P^o_{3/2})$	4677.0	4685.28	6.118	7.359	5446.84	2756
20 b	$1s2p^2(^2P_{3/2}) \rightarrow 1s^22p(^2P^o_{1/2})$	4677.0	4685.30	0.2116	0.2546	5446.84	2756
21 m	$1s2p^2(^2S_{1/2}) \rightarrow 1s^22p(^2P^o_{3/2})$	4697.7	4705.47	2.753	3.326	5467.02	2774
22 n	$1s2p^2(^2S_{1/2}) \rightarrow 1s^22p(^2P^o_{1/2})$	4697.7	4704.73	0.1301	0.1571	5467.02	2774

examine the individual $\sigma_{RC}(nJ\pi)$ in detail. The peak positions of 22 DES lines are listed in Table 1 for Fe XXIV, Ni XXVI and Ca XVIII along with S_{RC}, α_R, and $S(s)$, for Fe XXIV.

References

Bates, D. R., & Dalgarno, A. 1962, *Atomic and Molecular Processes*, ed. D.R. Bates (New York: Academic Press), p. 245
Beiersdorfer, P., et al. 1992, Phys. Rev. A, 46, 3812
Bely-Dubau, F., et al. 1982, MNRAS, 198, 239
Gabriel, A. H. 1972, MNRAS, 160, 99
Nahar, S. N., & Pradhan, A. K. 1994, Phys. Rev. A, 49, 1816
Nahar, S. N., & Pradhan, A. K. 2006, Phys. Rev. A, 73, 062718-1
Vainshtein, L.A., & Safronova, U.I. 1978, At. Data Nucl. Data Tables, 25, 49
Zhang, H. L., Nahar, S. N., & Pradhan, A. K. 1999, J. Phys. B, 32. 1459